ISSN (Print) 1226-1750
ISSN (Online) 2233-6656
Journal of Magnetics 24(4), 583-592 (2019) https://doi.org/10.4283/JMAG.2019.24.4.583

Research on Temperature Field of a New Type of Magnetorheological Fluid Dynamometer with Cooling System

Lei Wang, YiPing Luo*, Hui Ying Liang, and Meng Ji

College of Mechanical and Automotive Engineering, Shanghai University of Engineering Science, Shanghai 201620, China

(Received 5 August 2019, Received in final form 25 November 2019, Accepted 29 November 2019)

In order to study the temperature characteristics of magnetorheological fluid dynamometer, the torque model and working principle of magnetorheological fluid dynamometer were analyzed, the temperature experiment of magnetorheological fluid dynamometer was conducted, and the experimental data were analyzed and processed in this paper. The fitting curves between the speed of magnetorheological fluid dynamometer and the experimental temperature, the speed and the torque, the current and the torque as well as the current and the temperature were obtained. Then, the temperature field of magnetorheological fluid was simulated by FLUENT based on the experimental data. The temperature field nephograms and temperature values of test points under different working conditions were obtained. Comparing the experimental values with the simulation values, the relative error was less than 7.8 %, which was within a reasonable range. Finally, from the aspect of temperature reduction, the simulation model was optimized. Based on the principle of heat convection, the simulation model was reconstructed. The maximum temperature drop was 10 ^{o}C.

Keywords : magnetorheological fluid, MRF dynamometer, temperature field, finite element simulation

1. Introduction

Hydraulic dynamometer, electric dynamometer and eddy current dynamometer are three main types of dynamometers used in current projects [1, 2]. The hydraulic dynamometer mainly controls through the regulation of water output, and has poor measurement accuracy. Its e loading reaction time is second order. The loading reaction time of electric dynamometer is milliseconds, but its structure is complex and its cost is high. The structure of eddy current dynamometer is relatively simple and stable, but its response time is second order. Magnetorheological Fluid (MRF) is a new type of intelligent material, which consists of suspension with controllable rheological properties, and disperses from carrier (fine magnetic particles) to carrier (base fluid). Under the action of magnetic field, the viscosity of MRF can change continuously and it can change reversibly between Newtonian fluid and Bingham fluid instantaneously (in milliseconds), and the shear yield stress increases linearly with the increase of magnetic field. It is a valuable attempt to apply MRF to dynamometer.

Magnetorheological fluid dynamometer uses magnetorheological fluid as its working medium, and relies on the shear stress of interfacial magnetorheological fluid to transfer power. The shear yield stress can be controlled quickly and accurately by adjusting the intensity of external magnetic field. As a new application of magnetorheological fluid [3, 4], the magnetorheological fluid dynamometer has the characteristics of simple structure, rapid and reversible reaction, simple control, low energy consumption, low noise, low vibration and strong anti-interference ability. Magnetorheological fluids are widely used in many devices because of their magnetorheological properties. Neelakantan [5] designed the magnetorheological clutch and studied the influence of particle centrifugal force on its performance; Kavlicoglu [6] designed the multi-disk magnetorheological fluid limited slip clutch and eliminated the adverse effects of particle centrifugal force; Kikuchi [7, 9] designed a micro-structure. The thickness of gap rheological brake is only 50 microns; Sarkar [10] designed a single-disk extrusion magnetorheological fluid brake from the angle of magnetorheological fluid extrusion enhancement.

When the magnetorheological dynamometer works in shear mode, its kinetic energy is converted into thermal

*Corresponding author: Tel: +8613801933171
Fax: +8613801933171, e-mail: lyp777@sina.com

energy, which makes the temperature of the device rise and affects the rheological properties of magnetorheological fluids. Xiangfan Wu *et al.* [11] conducted the temperature field test of magnetorheological fluids, and found that when the temperature was higher than 100 ℃, the shear yield stress decreased rapidly due to thermal expansion and thermal magnetization effect. The performance of MRF device greatly deteriorated. Therefore, it was necessary to analyze the temperature field of dynamometer to ensure its normal operation. Many studies have shown that there is an obvious correlation among heat transfer coefficient and shear stress and temperature [12, 13]. Zheng Di [14] *et al.* used ANSYS to analyze the temperature field of the rotating MRF damper, based on which the cooling system of the device was designed and verified by experiments. Wang [15] designed a magnetorheological fluid brake with cooling system, which had a large torque, studied the influence of temperature on the torque and proved the importance of cooling system. Ghaednia *et al.* [16] used Newmark finite element method to analyze the influence of temperature on MRF squeeze film damper. The influence of temperature on the operation of MRF dynamometer has not been taken into account in the current research. Therefore, it is necessary to analyze the temperature distribution and temperature characteristics of MRF dynamometer, so as to provide theoretical basis for the optimal design of the device.

To conclude, from the angle of magnetorheological fluid transmission, the temperature experiment of the existing magnetorheological fluid dynamometer was carried out. Then, the temperature field of the dynamometer was analyzed by ANSYS simulation method and the simulation results were verified by experimental data. Finally, the magnetorheological fluid dynamometer was tested from the angle of natural convection and strong convection and structural design was optimized.

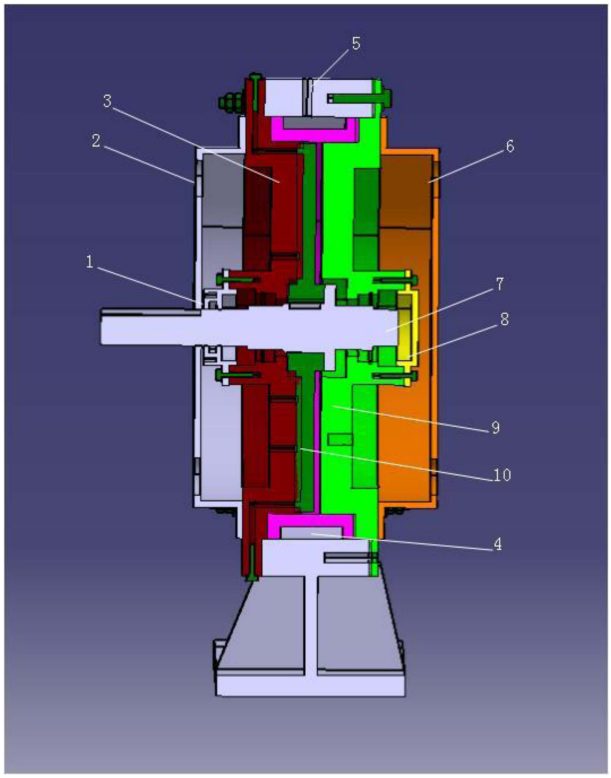

1—End cover, 2—Water jacket with hole, 3—Left shell, 4—Coil, 5—Outer ring, 6—Water jacket without hole, 7—Axis, 8—Water jacket without hole, 9—Right shell, 10—Rotary table

Fig. 1. (Color online) Structure of MRF dynamometer.

Table 1. The material of MRF dynamometer.

Structure	Material	Magnetism
Disk, Shell, Outer ring, The coil bracket	Q235-A	Magnetic material
Transmission shaft, End cover, Roller bearing end cap	1Cr18Ni9Ti	Non-magnetic material

2. Structure and Torque Model of Magnetorheological Fluid Dynamometer

2.1. Structure Model of Magnetorheological Fluid Dynamometer

The structure of MRF dynamometer is shown in Fig. 1, and its materials are shown in Table 1. MRF dynamometer is mainly composed of left and right shells, MR fluid, transmission shaft, rotary table, coil, outer ring, bearing, water jackets, etc. The drive shaft is connected with the motor, and the rotating disc is fixed on the drive shaft by screw. The coil is surrounded by the left and right shells along the radial direction, and the magnetorheological fluid is in the gap between the left and right shells and the rotary table. When the coil is electrified, the gap between magnetorheological fluids will produce an axial magnetic field. The water jacket with hole is installed on both sides of the left and right shells. The water jackets are connected with both pumps and radiators to reduce the temperature field of dynamometers.

2.2. The Torque Model of MRF Dynamometer

d_r is a tiny cell in the disk, r is radius of the tiny cell, r and R are inner radius and outer radius of the disk, respectively, and ω_r is the angular speed of the disk, as shown in Fig. 2.

The shear force of the tiny cell should satisfy

$$dF = \tau \cdot dA = \tau 2\pi r dr \tag{1}$$

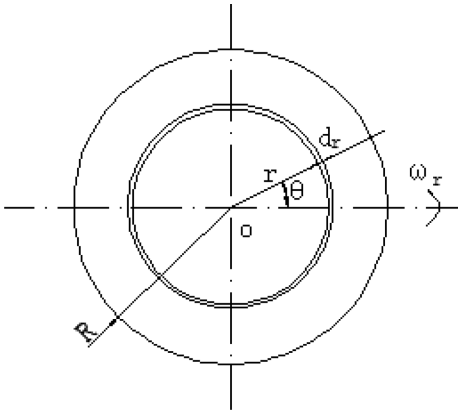

Fig. 2. Calculation model of torque.

The torque of the tiny cell should satisfy

$$dT = r \cdot dF = 2\pi r^2 \tau dr \tag{2}$$

The shear strain rate should satisfy

$$\gamma = r \cdot \frac{\omega_2 - \omega_1}{h} \tag{3}$$

where h is the working gap between disk and shell, r is the radius of the tiny cell, ω_1 and ω_2 are angular speeds of shell and disk respectively.

The binham constitutive equations of MRF are:

$$\begin{cases} \tau = \tau_B \operatorname{sgn}(\gamma) + \eta\gamma & |\tau| \geq \tau_B \\ \gamma = 0 & |\tau| < \tau_B \end{cases} \tag{4}$$

$$\gamma = r\frac{d\omega}{dr} \tag{5}$$

where τ is sheer stress of MRF, τ_B is sheer yield stress of MRF, η is dynamic viscosity of MRF, and γ is sheer strain rate of MRF.

Formulas (3) and (4) generate formula (2)

$$dT = 2\pi r^2 \left(\tau_B + \eta \frac{\omega_2 - \omega_1}{h} r \right) dr \tag{6}$$

Formula (4) is torque based on an integral

$$\begin{aligned} T &= \int_r^R 2\pi r^2 \tau dr \\ &= 2\pi \int_r^R r^2 \left(\tau_B + \eta r \frac{\omega_2 - \omega_1}{h} \right) dr \\ &= \left(\frac{2\pi}{3} \tau_B r^3 + \frac{1}{2h} \pi\eta\omega r^4 \right) \Big|_r^R \\ &= \frac{2\pi}{3} \tau_B (R^3 - r^3) + \frac{\pi\eta\omega}{2h} (R^4 - r^4) \end{aligned} \tag{7}$$

The torque of the prime mover is generated by the motor, and the torque generated by the prime mover is absorbed and measured by the magnetorheological dynamomete. According to formula (7): the torque of MRF dynamometer consists of two parts, which are T_B, the magnetic torque generated by MRF sheer yield stress, and T_η, the viscous torque generated by MRF inherent viscidity. T_η is much smaller than T_B, so the torque of MRF dynamomter depends on the magnetic torque.

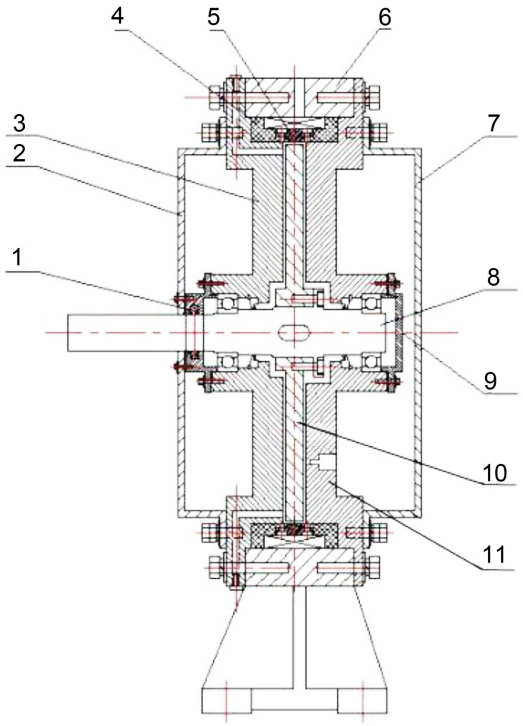

1—plate with hole, 2—Water jacket with hole, 3—Left shell, 4—Coil, 5—Magnetic isolation ring, 6—Outer ring, 7—Water jacket with hole, 8—Axis, 9—Water jacket without hole, 10—Rotary table, 11—Right shell

Fig. 3. (Color online) Schematic view of MRF dynamometer structure.

2.3. The Working Principle of MRF dynamomter

As shown in Fig. 3, the magnetorheological fluid dynamometer mainly adopts the shear mode of magnetorheological fluid, and its structure adopts the disc type. When the coil is not electrified, the magnetorheological fluid presents as Newtonian fluid, and the active disk rotates only under the influence of viscous resistance in the fluid.

When the coil is electrified, the working area generates magnetic field along the rotating axis, and the magnetorheological fluid presents as Bingham fluid. Magnetorheological fluid contains magnetic particles which form a chain connecting the head and the tail in the direction of magnetic field. When the rotary table rotates, the flux is

sheared. The torque absorbed by the dynamometer is determined by the shear strength of the flux. Before the flux reaches saturation, the shear strength increases with the increase of the magnetic field strength. When the excitation current is large enough, the flux linkage reaches saturation, and the shear strength does not increase with the increase of the magnetic field strength.

3. Temperature Field Test of Magnetorheological Fluid Dynamometer

As shown in Fig. 4, the temperature test bench of dynamometer is built, and the temperature field test bench of magnetorheological dynamometer is controlled by adjusting the parameters (speed and current) on the panel of electric control cabinet. The motor is connected with the rotary table of magnetorheological fluid dynamometer through the torque and speed sensor and coupling. The electric control system controls the frequency converter to adjust the speed of the motor. During the rotating process, the rotary table shears the magnetorheological fluid flux formed under the action of magnetic field, and heat energy generates, so the temperature field of dynamometer increases. Finally, the temperature field of dynamometer is controlled by a cooling system composed of water jacket, radiator, water tank and water pump.

The location of temperature test point of MRF dynamometer is shown in Fig. 5.

The temperature sensor of dynamometer (PT100, Shanghai Songdao Heating Sensor Co., Ltd.) and its temperature test point are located in its right shell. The distance between the probe of temperature sensor and MRF is very small. Therefore, the temperature value measured by the probe of temperature sensor can be approximately regarded as the temperature of MRF. Tables 2 and 3 are the

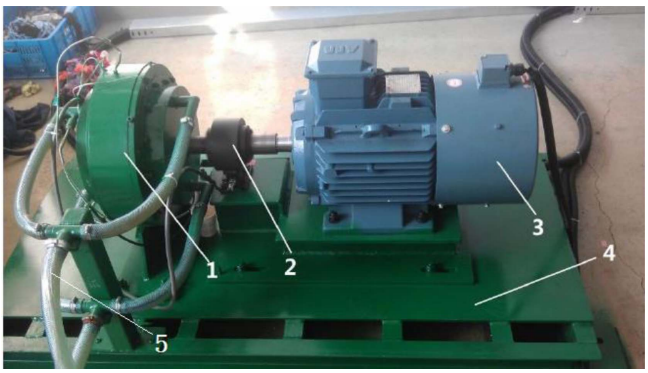

1—Dynamometer, 2—Torque speed sensor, 3—Electrical machine, 4—Pedestal, 5—Cooling system

Fig. 4. (Color online) Test bench spot of MRF dynamometer.

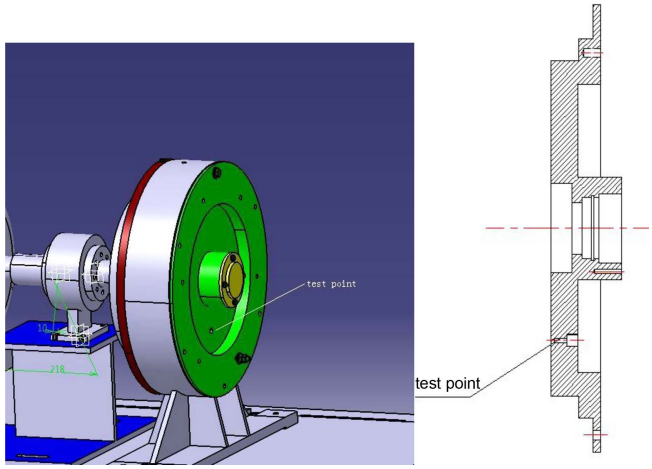

Fig. 5. (Color online) Location of temperature test point.

Table 2. temperature and speed test.

Testprocedure	Current (A)	Speed (r/min)	Control time (mins)
Initialposition	0	0	0
Preheat	0.17	100	5
Increase speed	0.17	500~2500	20
Decrease speed	0.17	2500~500	20

Table 3. temperature and current test.

Testprocedure	Current (A)	Speed (r/min)	Control time (mins)
Initialposition	0	0	0
Preheat	0.17	100	5
Increase speed	0.17	100~1700	10
Increase current	0.17~1.49	1700	30
Decrease current	1.49~0.17	1700	30
Decrease speed	0.17	100	10

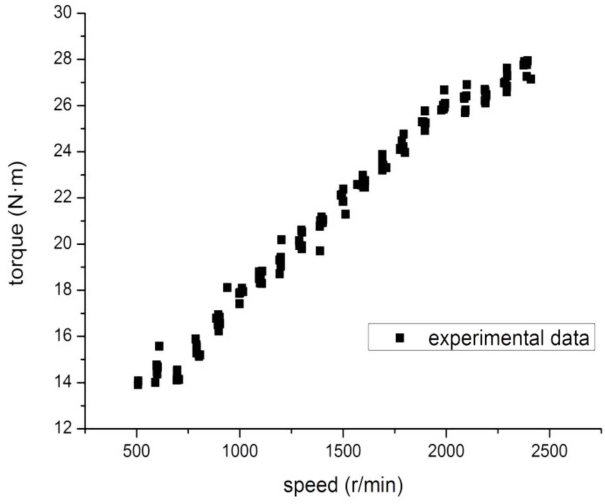

Fig. 6. Relationship between speed and rotate without MRF.

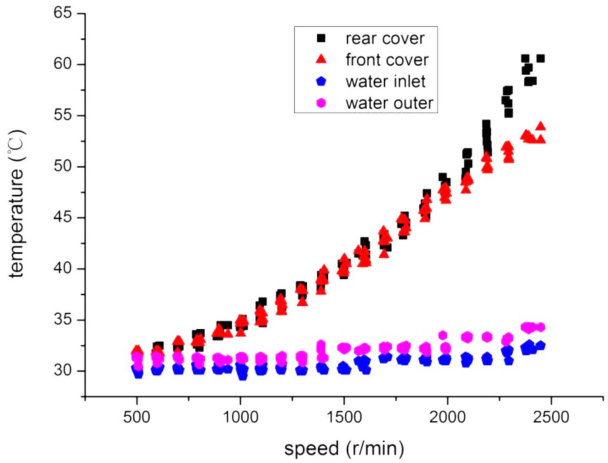

Fig. 7. (Color online) Relationship between test temperature and rotate speed with MRF.

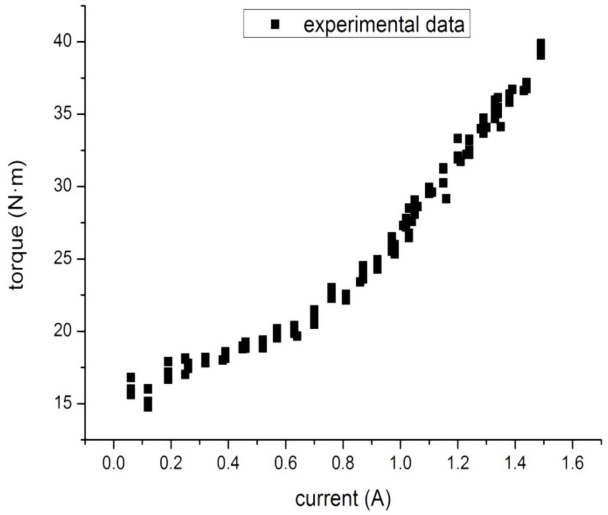

Fig. 8. Relationship between current and rotate with MRF at 1700 RPM.

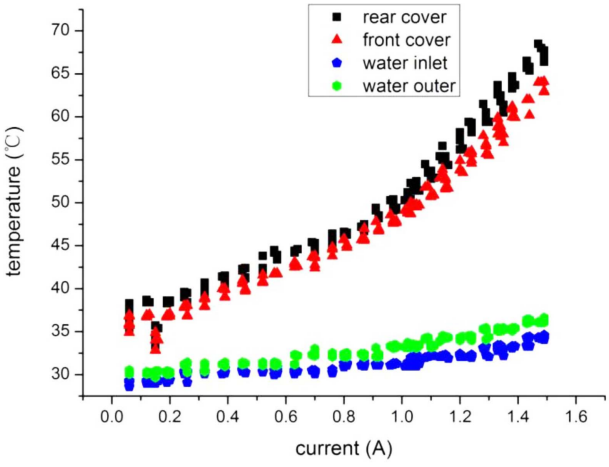

Fig. 9. (Color online) Relationship between current and temperature with MRF at 1700 RPM.

steps of the test. The relationships among speed, torque, temperature and current obtained from the test are shown in Figures 6, 7, 8 and 9.

As shown in Fig. 6, the torque of dynamometer increases with the increase of rotational speed, and it can be seen from Fig. 7 that the temperature of the test point of magnetorheological fluid dynamometer increases with the increase of rotational speed. There is a positive correlation among speed, torque and temperature, and the highest temperature is 60.25 °C. Fig. 8 shows that under the fixed speed of 1700 r/min, the torque increases with the increase of current, and the maximum is 40.06 N·m. It can be seen from Fig. 11 that the temperature increases with the increase of current when the speed is 1700 r/min, and the highest temperature is 67.57 °C. The temperatures of the back end and the front end change obviously with the rotational speed. The temperatures of the inlet and the outlet increase with the rotational speed, but the trend is very small.

During the test, the data acquisition system collects a lot of data, such as temperature (temperatures of test point, inlet and outlet, water tank), rotational speed and torque. The temperatures of inlet and outlet, temperature

Table 4. Experimental data.

Test temperature (ºC)	Outer temperature (ºC)	Tank temperature (ºC)	Inner temperature (ºC)	Speed (r/min)	Torque (N·m)
61.65	34.35	32.05	32.00	2393.5	31.64
56.33	33.20	31.83	31.27	2185.67	30.56
51.20	33.33	32.03	31.23	1923.67	29.18
46.20	32.23	30.97	31.40	1687.33	27.59
41.28	32.33	31.05	30.33	1378.5	24.52
36.66	32.16	30.94	31.24	962.2	20.59

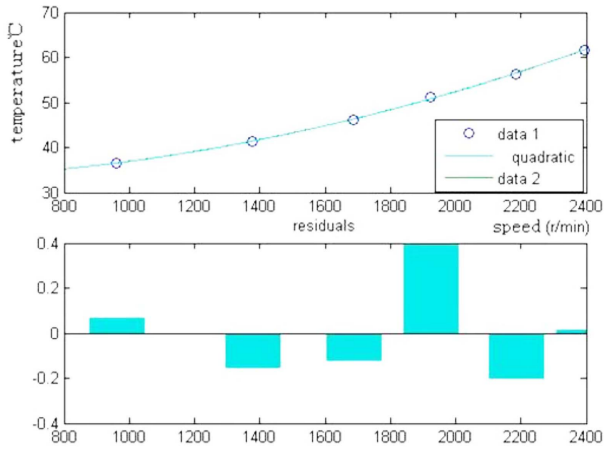

Fig. 10. (Color online) Fitting curve of speed and temperature.

of water tank, rotational speed and torque are the boundary conditions of ANSYS (FLUENT) analysis. The temperature data of the test point are used for verification. The correctness of temperature field model of magnetorheological fluid dynamometer can ensure the correctness of temperature cloud and simulation temperature at test point, as shown in Table 4.

Using MATLAB to fit the temperature of the test point shown in Fig. 10, the fitting function between the temperature and the speed of the test point can be obtained. It can be clearly seen that the relationship between the speed and the temperature of the test point is linear, and the higher the speed is, the higher the temperature is.

Simulation result:

$$T_{temperature} = 5.8\times10^{-6}n^2 - 0.0019n + 33 \quad (800r/\min \le n \le 2400r/\min) \tag{8}$$

4. Simulation Analysis

4.1. Governing Equations

4.1.1. Heat Conduction Differential Equation

The internal temperature distribution law of magnetorheological fluid dynamometer can be represented with equation (9):

$$\frac{\partial}{\partial x}\left(k_{xx}\frac{\partial T}{\partial x}\right)+\frac{\partial}{\partial y}\left(k_{yy}\frac{\partial T}{\partial y}\right)+\frac{\partial}{\partial z}\left(k_{zz}\frac{\partial T}{\partial z}\right)+\dot{\Phi}_V=\rho c\frac{dT}{dt} \tag{9}$$

where $\dot{\Phi}_V$ is calorific power per unit volume of MRF, ρ is the density of material, c is the heat capacity of material, k_{xx}, k_{yy} and k_{zz} are coefficients of thermal conductivity of x, y and z respectively.

4.1.2. The Calculation of Heat Generation Rate

Average calorific value per unit volume of MRF can be described by equation (10).

$$\dot{\Phi}_{VA}=\frac{\mathrm{P}}{V}=\frac{M\omega}{V}=\frac{2}{3}\frac{R^3-r^3}{R^2-r^2}\frac{\tau\omega}{h} \tag{10}$$

where P is power, ω is angular speed, V is volume of MRF, M is torque, h is working distance, r and R are inner radius and outer radius of the disk respectively, and τ is sheer yield stress.

4.1.3. FEM Model

Assuming that the physical properties of metal materials of magnetorheological fluid dynamometer do not change with temperature and the boundary conditions change, the differential equation changes to:

$$[C]\{\dot{T}\}+[K]\{T\}=\{Q\} \tag{11}$$

Table 5. Boundary condition.

Hear source intensity (W/m^3)	Export water temperature (^oC)	Import water temperature (^oC)
3.2×10^7	34.35	32
2.82×10^7	33.2	31.27
2.37×10^7	33.33	31.23
1.97×10^7	32.23	31.4
1.43×10^7	32.33	30.33

Table 6. Magnetorheological fluid physical properties.

Structure	Material	Density (kg/m^3)	Coefficient ($W/m^2\cdot K$)	Specific heat ($J/(kg\cdot K)$)
Water jacket without hole	1Gr18Ni9Ti	7850	18	460
Cover without hole	1Gr18Ni9Ti	7850	18	460
Right shell	Q235A	7800	52	486
Outer ring	Q235A	7800	52	486
Enameled wire	Cu	8900	393	390
Coil	Q235A	7800	52	486
MRF	MRF	3000	1	1000
Disk	Q235A	7800	52	486
Axis	1Gr18Ni9Ti	7850	18	460
Left shell	Q235A	7800	52	486
End cover with hole	1Gr18Ni9Ti	7850	18	460
Water jacket with hole	1Gr18Ni9Ti	7850	18	460
Air	air	0.946	0.0321	1009

where $[K]$ is the transmission matrix which includes oefficient of thermal conductivity and convection coefficient, $[C]$ is specific heat matrix, $\{T\}$ is the node temperature vector, $\{\dot{T}\}$ is the derivative of temperature to time, and $\{Q\}$ is heat flow rate vector of nodes.

4.1.4. Boundary Condition and Calculation Parameter

The boundary conditions of this model are velocity inlet boundary condition (the speed and scalars of the entry are defined), pressure outlet boundary condition (outlet static pressure is defined) and convective heat transfer wall surface (thermal conductivity, fluid temperature). The accurate data are shown in Table 5 and Table 6.

4.2. Simulation and Analysis

The simplified physical model of dynamometer is shown in Fig. 11. Different working conditions of the magnetorheological fluid dynamometer are simulated and analyzed by using FLUENT. The simulation value of test point is shown in Table 7. The simulation results are shown in Fig. 12. The fitting curve between simulation

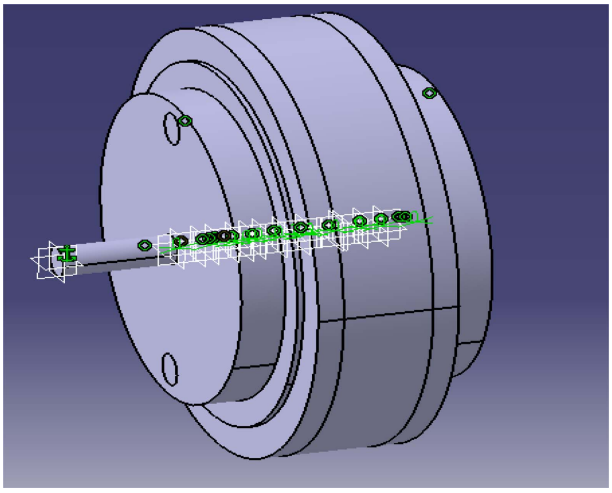

Fig. 11. (Color online) Physical model of dynamometer.

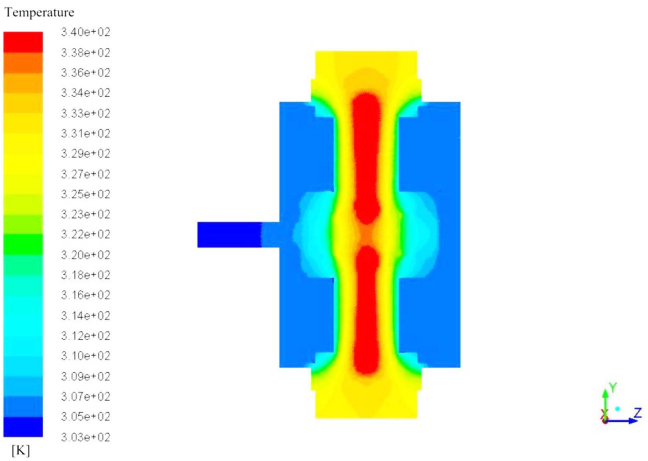

Fig. 12. (Color online) P=7936.13W temperature nephogram.

temperature and speed of the dynamometer test point is obtained by using MATLAB, as shown in Fig. 13.

It can be seen from Fig. 12 that the temperatures of magnetorheological fluid and rotary table are high, while the temperature of the outer end of the spindle is low. The reason for this phenomenon is that the magnetorheological fluid produces shear stress under the action of external magnetic field, and the kinetic energy of dynamometer is entirely transformed into the thermal energy of magnetorheological fluid, which means the magnetorheological fluid becomes the heat source, so the magnetorheological fluid connects with it. The temperature at the contact point is high. However, the left and right shells contact with the cooling water which takes part of the heat away, so the temperatures of the left and right shells are not very high. The outer surface of the outer ring contacts with the air and there is natural convection at the contact surface, so the temperature of the outer ring is low, and

Table 7. Temperature and error of test point.

Number	Speed (r/min)	Power (W)	Test (℃)	Simulation (℃)	Absolute error (℃)	Relative error (%)
1	2393.50	7936.13	61.65	63.85	2.20	3.5
2	2185.67	6993.16	56.33	59.35	3.02	5.4
3	1923.67	5877.98	51.20	54.85	3.65	7.1
4	1687.33	4874.69	46.20	49.65	3.45	7.5
5	1378.50	3540.38	41.28	43.70	2.42	5.9
6	962.20	2075.11	36.66	38.85	2.19	6.6

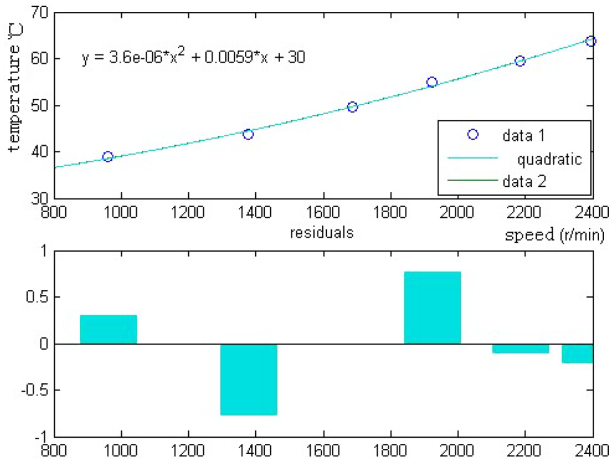

Fig. 13. (Color online) Fitting curve between speed and simulation temperature.

the coil and the rotating shaft contacting with the magnetorheological fluid have a very high temperature. The outer end contacts with the air, so its temperature is also low.

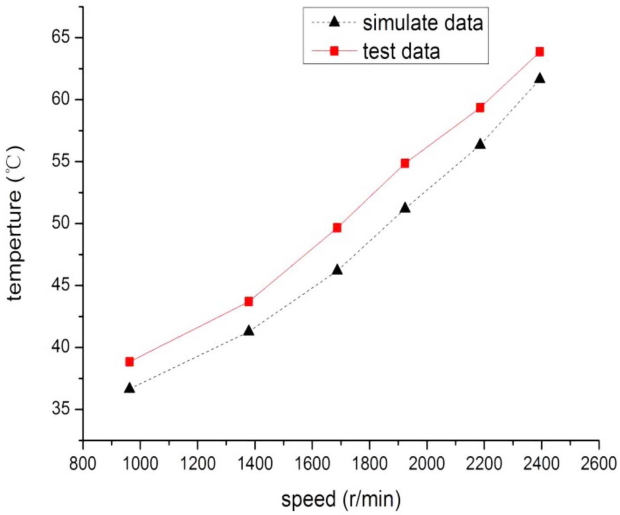

Fig. 14. (Color online) Experiment and simulation of temperature curve fitting.

The temperature field test data of the dynamometer are compared with the simulation data of the test point at different working conditions, and the comparison results are shown in Table 7.

The simulation temperature of test point of MRF dynamometer is fitted using MATLAB and the fitting function between speed and simulation temperature is shown in Fig. 13.

Fitting results:

$$T_{simulation} = 2.5\times10^{-6}n^2 + 0.0094n + 27 \quad (800r/\min \le n \le 2400r/\min) \tag{12}$$

$$T_{simulation} - T_{test} = -3.3\times10^{-6}n^2 + 0.0113n - 6 \quad (800r/\min \le n \le 2400r/\min) \tag{13}$$

Fig. 14 is a broken-line chart, which compares the temperature field test data of dynamometer with the simulation data of the test point at different working conditions. According to formula (13), the absolute error reaches the maximum value of 3.67 when n = 1713 (r/min). The test temperature is 47.09 °C at n = 1713 (r/min). The relative error at n = 1713 (r/min) is 7.8 %. In engineering practice, it is considered that the error within 10 % is acceptable. The errors are within a reasonable range, so the temperature field model of MRF dynamometer is correct.

5. Simulation Optimization

The temperature distribution law obtained by the experiment is basically the same as that obtained by the numerical simulation, but there are still some errors, which are mainly caused by the simplification of the simulation model and boundary conditions, the nonlinearity of the thermal physical properties of the transmission material and the measurement error of the temperature sensor. In order to reduce the temperature of the device, considering the natural convection and forced convection, the distance between the contact surface and the heat source (magnetorheological fluid) can be reduced, that is, the diameters of the outer ring and the left and right shells can be reduced, or the thickness of the left and right shells can be reduced.

5.1. Natural Convection Optimization

The outer surfaces of the left shell and the right shell of MRF dynamometer are in contact with air. There is natural convection heat transfer on the contact surface, which affects the temperature field of the dynamometer. In order to reduce the temperature of the device, the distance between the contact surface and the heat source (magnetorheological fluid) can be reduced, that is, the diameters of the outer ring and the left and right shells can be reduced. As shown in Fig. 15, a new structure model 1 is re-constructed. The variations of the specific parameters are shown in Table 8.

Table 8. Parameters of the optimization.

Structure	Diameter of initial model T (mm)	Diameter of model one T (mm)
Left shell	400	370
Right shell	400	370
Cover	400	370

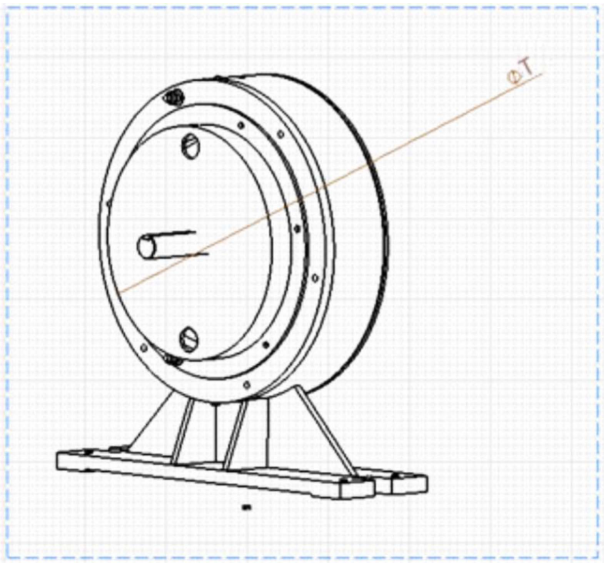

Fig. 15. (Color online) Reconstructed structure model 1.

The physical field model (model 1) is shown in Fig. 15. The temperature field of model 1 is simulated by ANSYS. The temperature cloud and the temperature value at the

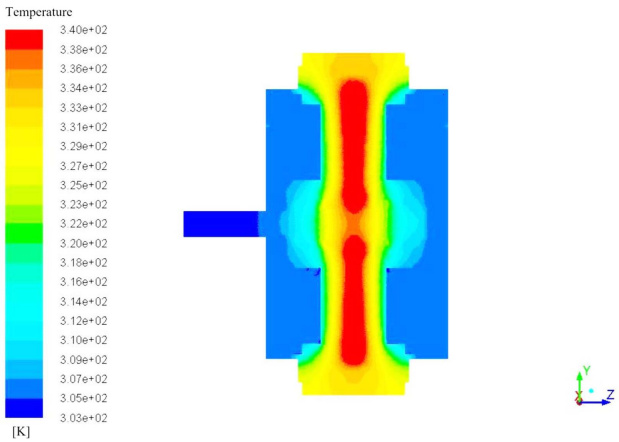

Fig. 16. (Color online) P = 7936.13 W temperature nephogram of model 1.

Table 9. Parameters of the optimization.

Structure	Thickness of initial model D (mm)	Thickness of model two D (mm)
Left shell	25	15
Right shell	25	15

test point obtained are shown in Fig. 16. Then, the temperature values at the test point of the dynamometer before and after changing the model are compared.

The temperature cloud of the new model (model 1) of MRF dynamometer has the same trend as that of the original model. The temperature of the test point of the optimized model is 61.85 ℃, which is 2 ℃ lower than that of the original model.

5.2. Forced Convection Optimization

The cooling system of magnetorheological fluid dynamometer test bench is a forced convection heat transfer system. The forced convection heat transfer takes away a lot of heat, so the cooling system has a great influence on the temperature of dynamometer. The left and right shells are between the cooling water and the magnetorheological fluid, and their thickness has a great influence on the temperature distribution of the device. In order to reduce the temperature of the magnetorheological fluid dynamometer, the thickness of the left and right shells can be reduced. As shown in Fig. 17, the variations of specific parameters are shown in Table 9.

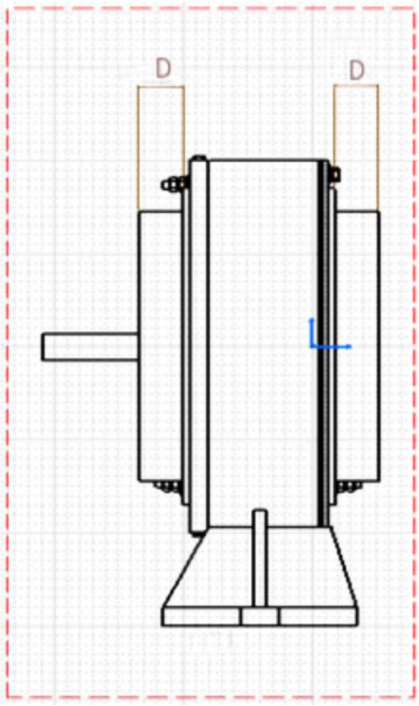

Fig. 17. (Color online) Reconstructed structure model 2.

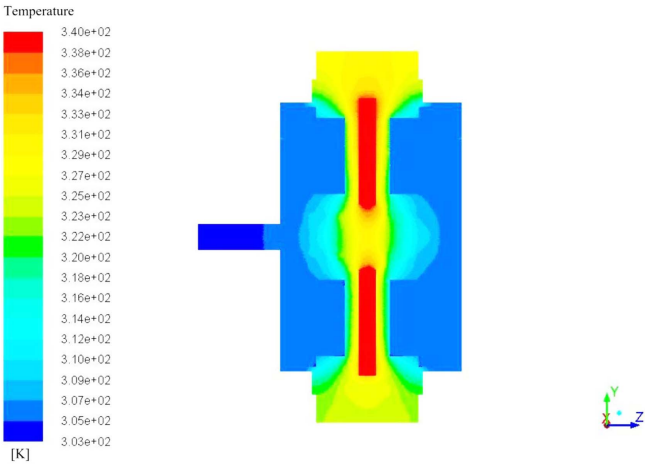

Fig. 18. (Color online) P = 7936.13 W temperature nephogram of model 2.

A new physical model (model 2) of MRF dynamometer is re-constructed in Fig. 17. The temperature field of MRF dynamometer is simulated by ANSYS. The temperature cloud and the temperature value at the test point obtained are shown in Fig. 18. The temperature value of the test point of the original model is compared with that of the optimized model.

The temperature cloud of the new model (model 2) of MRF dynamometer has the same trend as that of the original model. The test point temperature of the optimized model is 53.85 ℃, which is 10 ℃ lower than that of the optimized model.

6. Conclusion

Firstly, the MRF dynamometer bench was built by using the existing MRF dynamometer. Secondly, the temperature experiment of dynamometer was carried out, and the fitting curve between the speed of magnetorheological dynamometer and the temperature of the test point was obtained. The relationships between speed and torque, current and torque, current and temperature were also obtained. Then, the temperature field of magnetorheological fluid is simulated by FLUENT based on the data obtained from the experiment. The temperature field clouds and temperature values of test points at different working conditions were obtained. The simulation and experiment were compared to verify the correctness of the temperature field model of the MRF dynamometer. Finally, based on the temperature field model, the temperature field of dynamometer was simulated and optimized from the aspects of natural convection and forced convec-

tion. On the basis of this study, the following conclusions can be drawn: In the case of fixed current, the temperature increases with the increase of speed, and the torque increases with the increase of speed; in the case of fixed speed, the temperature increases with the increase of current; the torque and current are positively correlated with speed.

(1) Both the temperature and the torque increase with the increase of speed under the condition of a fixed current; The temperature increase with current under the condition of a fixed speed; Both the torque and current have a positive correlation with speed.

(2) The simulation results of magnetorheological fluid dynamometer show that the temperatures of magnetorheological fluid and rotary table are high while the temperature of spindle exterior is low, and the error of temperature simulation data of test point is less than 7.8 %.

(3) Based on the optimization of natural convection, simulation results show that the temperature of the test point of the optimized model is 2 ℃ lower than that of the optimized model; based on the optimization of forced convection, simulation results show that the temperature of the test point of the optimized model is 10 ℃ lower than that of the optimized model.

Acknowledgement

The support of Science and Technology Commission of Shanghai Municipality (Grant No. 19030501100).

References

[1] P. Fajri, S. Lee, V. A. K. Prabhala, *et al.* Modeling and Integration of Electric Vehicle Regenerative and Friction Braking for Motor/Dynamometer Test Bench.
[2] D. K. Kang and M. S. Kim, International Journal of Automotive Technology **16**, 1031 (2015).
[3] D. H. Wang and W. H. Liao, Smart Materials and Structures **20**, 023001 (2011).
[4] O. Erol, B. Gonenc, D. Senkal, *et al.*, J. Intell. Mater. Syst. Struct. **23**, 427 (2012).
[5] V. A. Neelakantan and G. N. Washington, J. Intell. Mater. Syst. Struct. **16**, 703 (2005).
[6] N. C. Kavlicoglu, B. M. Kavlicoglu, Y. M. Liu, C. A. Evrensel, *et al.*, Smart Mater. Struct. **16**, 149 (2007).
[7] T. Kikuchi, K. Ikeda, K. Otsuki, T. Kakehashi, *et al.*, J. Phys.: Conf. Ser. **149**, 012059 (2009).
[8] T. Kikuchi, K. Otsuki, J. Furusho, H. Abe, *et al.*, Adv. Robot. **24**, 1489 (2010).
[9] T. Kikuchi, K. Kobayashi, and A. Inoue, J. Intell. Mater. Syst. Struct. **22**, 1677 (2011).
[10] C. Sarkar and H. Hirani, Smart Mater. Struct. **22**, 115032 (2013).
[11] Xiangfan Wu, Master. Thesis, China University of Mining and Technology (2017).
[12] Y. Gokhan and G. Seval, Smart Mater. Struct. **22**, 1 (2013).
[13] O. G. H. M. Murat, Rheol. Acta. **52**, 623 (2013).
[14] D. Zheng, W. C. Ye, L. Y. Hu, *et al.*, 2009 IEEE ASME International Conference on Advanced Intelligent Mechatronics [C]. Singapore, SINGAPORE, IEEE; ASME, P.42-46.
[15] D. M. Wang, Master. Thesis, China University of Mining and Technology (2014).
[16] H. Ghaednia and A. Ohadi, J. Vib. Acoust. **134**, 1 (2012).